ASIAN JOURNAL OF PHARMACEUTICAL AND CLINICAL RESEARCH

INNOVARE ACADEMIC SCIENCES
Knowledge to Innovation

Vol 8, Issue 4, 2015

ISSN - 0974-2441

Research Article

INSIGHT INTO THE MOLECULAR INTERACTION OF ANTI MALARIAL COMPOUNDS AS POTENTIAL CHORISMATE SYNTHASE INHIBITORS

SAJITHA LULU S[1], THABITHA A[1], MOHANA PRIYA A[1], VINO S[2]*

[1]Bioinformatics Division, School of Bio Sciences and Technology, VIT University, Vellore - 632 014, Tamil Nadu, India.
[2]Medical Biotechnology Division, School of Bio Sciences and Technology, VIT University, Vellore - 632 014, Tamil Nadu, India.
Email: svino@vit.ac.in

Received: 11 January 2015, Revised and Accepted: 24 March 2015

ABSTRACT

Objective: The study is focused and directed towards a promising gateway for novel inhibitor designing against malaria.

Methods: Homology model was built for both ON-state and OFF-state of *Plasmodium falciparum* chorismate synthase (PfCS) protein. Around 240 antimalarial compounds were docked into the active site of PfCS to understand the interaction and binding affinity. Virtual screening was carried out based on docking score, molecular properties, drug likeliness and bioactivity toward lead molecule selection.

Results: Based on these properties out of 240 compounds, we found the best fit ligand idarubicin interacting with Arg46, Lys60, Glu86, Arg483 and Arg491 of ON state PfCS, with a high docking score of -13.7. The stability of complex and hydrogen bonds were analysed with molecular dynamic simulations. In OFF state also idarubicin interacting with a docking score of -15.2 and interacting residues was found to be Ser16, Glu86, Gly126, Arg127 and Arg491.

Conclusion: Malaria, a cataclysmic disease caused by protozoan parasite *P. falciparum* is a leading disease and cause of death in many of the developing countries. CS is an enzyme, which plays a major role in the aromatic amino acid biosynthesis of the shikimate pathway. Inhibition of PfCS protein is reported to affect the growth and survival of the parasite. In this study, idarubicin compound shows anti-parasitic activity and high binding affinity towards PfCS.

Keywords: Homology model, Drug likeliness, Shikimate pathway, Idarubicin.

INTRODUCTION

Malaria is the third most deadly disease of the human system, and it emerges as a diagnostic and therapeutic challenge [1]. *Plasmodium falciparum* is the protozoan parasite which out of 5000 apicomplexan species affects more than 74% of the people in Africa and South-East Asia through blood-borne malarial disease worldwide [2-4]. In 2011, WHO estimated that 300-500 million cases are in diseased state, and 0.5 million deaths occur annually [5]. Perhaps the most widely used drugs are quinolines, antifolates and artemisinin derivatives [3]. A symptom of this disease is fever, chills, prostration and anemia, in the severe case can include delirium, metabolic acidosis, cerebral malaria and multi-organ system failure and coma. New, effective, less toxic and affordable antimalarial agent for increasing drug resistance strains of malaria are necessary to be developed through computational therapeutic approaches [6].

The shikimate pathway for aromatic biosynthesis is present in the cytosol of bacteria, fungi, plants and apicomplexan parasites, is absent in mammals. Chorismate synthase of *P. falciparum* (PfCS) reveals unique catalytic mechanism, which can act as attractive target for antimalarial drugs. The seventh and final step of shikimate pathway includes CS (EC 4.6.1.4), which converts 5-enolpyruvylshikimate-3-phosphate (EPSP) to chorismate and phosphate, with reduced flavin mononucleotide (FMN) molecule as a cofactor for redox neutral reaction [7]. CS catalyses the anti-1,4-elimination of phosphate and the C6-*pro*-R hydrogen of EPSP [8,9]. CS can act as a precursor for synthesis of aromatic aminoacids phenyl alanine, tryptophan and tyrosine, indole and its derivatives, 2,3-dihydroxybenzoic acid, antibiotics, ubiquinol and enterobactin biosynthesis, salicyclic acid, aromatic metabolites like alkaloids, folates, vitamin K and para-amino benzoate [10]. CS enzyme plays a critical role in the growth of *P. falciparum*. The shikimate pathway is also the target of the broad spectrum herbicide, glyphosate, and it also supplies folates to mammals which have recently been implicated in apicomplexan organisms such as malaria. The shikimate pathway believed to be absent from all protozoans was recently demonstrated to be present in apicomplexan parasites [11]. In the present study, we explored the potentials antimalarial agents through inhibiting a key enzyme of the shikimate pathway.

METHODS

Homology modeling and model validation

The PfCS sequence was obtained from NCBI protein database with accession no AAB63293.1.The templates were identified for homology modeling via BLASTp program against Protein Data Bank (PDB). (http://www.ncbi.nlm.nih.gov/BLASTp/). We used the monomer structures as templates extracted from the crystal structures of other organisms with more than 40% identity (Table 1). A multiple sequence alignment of PfCS sequence with two template protein sequence was constructed with ClustalW [12]. Multiple crystal structure proteins were used to build a multi-template three-dimensional (3D) model of the PfCS monomer using Modeller9v7 [13]. The model ligand module in the Modeller9v7 was used to model the FMNred bound PfCS structure; reduced FMN as a cofactor. Both FMNred bound (ON-state) and FMNred free (OFF-state) model of PfCS were modeled using same templates. We used the CS-HP-FMN crystal structure as the template for our FMNred bound modeling. The CS protein structure was also predicted using I-TASSER server. The modeled structures were then evaluated using the Procheck [14] and ProsA server [15] (Fig. 1).

Energy minimization and MD simulation

The CS protein (ON and OFF state) structures was further refined by the energy minimization and molecular dynamics simulation using

Table 1: Details of template sequences

Template ID	Identity (%)
IR52	46
4LJ2	43
IUM0	41

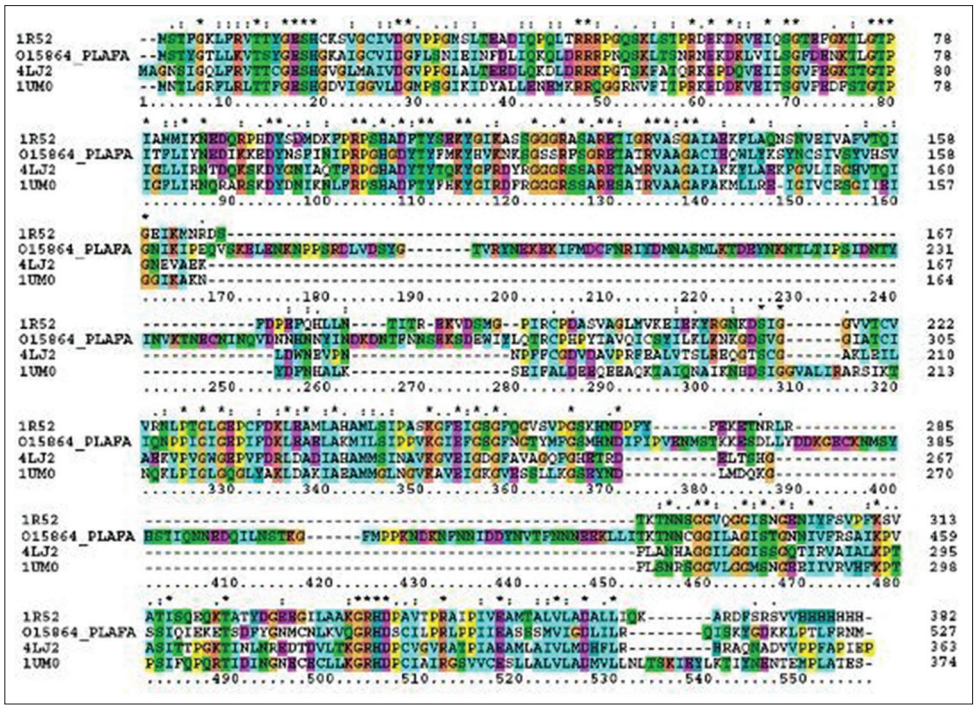

Fig. 1: Multiple sequence alignment of the target and template sequence

Gromacs 4.5.4 package with GROMOS96 43a1 force field [16]. The topology parameters of proteins were created by using the Gromacs program. The topology parameters of FMN were retrieved from PRODRG server. The predicted model was solvated in a truncated octahedron periodic box of simple point charge water molecules. The system was then energy minimized using a steepest gradient method for 10,000 steps and continuous with conjugate gradient method 10,000 steps. To equilibrate the system, position-restrained dynamics simulation of solute (NVT and NPT) at 300 K for 300ps. Then MD production was run at 300 K temperature and 1 bar pressure for 1 ns/1000ps.

Secondary structure prediction and active site prediction

The active site of PfCS has been predicted using Q-site finder. In Q-site finder the most favorable regions ranked based on the hydrophobicity of binding pocket. Secondary structure prediction was done with PSIPREDv3.3 online tool.

Ligand selection

The inhibitors that can act against CS protein were manually retrieved from Drugbank and Pubchem Databases. Around 240 compounds with antimalarial activity were selected for the *studies (Supplementary Table 1).*

Molecular docking

The possible interaction between ligand and receptor protein was studied using Auto dock Vina software [17]. The default parameters were used for this docking study. The coordinates of active sites obtained from Q-site finder were chosen to set grid box size. Lamarckian genetic algorithm was used to search for the best conformation of the docked protein-ligand complex. The log files were used to estimate the least binding energy for all the protein-ligand complexes. The binding modes of the ligand in the protein-ligand complex were visualized using pymol [18].

Drug Likeliness and bioactivity prediction

Virtual screening of the compounds was performed by using drug likeliness property with Lipinski's rule of five and physiochemical properties using molinspiration [19], cheminsilico server [20], XLOGP v2.0 and prediction of activity spectra for biologically active substances (PASS) server [21,22]. The PASS score for anti-parasitic and anti-protozoan activity were also taken into consideration for virtual screening.

RESULTS AND DISCUSSION

CS has a unique catalytic activity which is biochemically distinct hence this might lay the path for developing an effective and specific anti-parasitic agent. Nearly, more than 110 countries and territories were reported about the malarial transmission. These statistics indicates the severity of malaria as the pre-eminent disease, and it is one of the major killer transmissible diseases. Antimalarial drug resistance is recognized to be one of the greatest challenges to our ability against malaria. Selections of novel molecular targets as potential therapeutic drug targets are of paramount importance. With the increase in drug resistance, it becomes highly crucial to develop novel compounds to prevent the emergence of multidrug-resistant *P. falciparum*. Thus, it sounds to be inevitable to have a computational investigation using homology modeling and molecular docking towards designing inhibitors for CS.

Homology modeling

Homology modeling is also known as creating an atomic resolution model of the target protein from known tertiary structures of PDB database, which is conserved than amino acid sequences. CS catalyzes the conversion of EPSP to chorismate in the shikimate pathway, which represents an attractive target for discovering antimalarial agents. CS requires reduced FMN as a cofactor for catalysis. Hence, we modeled the structure of PfCS in both FMN-bound and FMN-free form (Fig. 2).

Template identification

The protein sequence of PfCS (527aa) was retrieved from NCBI database. BLASTp program was used for template search. Information of template sequences found with comparatively higher identity was identified and tabulated (Table 1).

Multiple sequence alignment

Multiple sequence alignment has been performed to discover common motif in the set of sequences. Identical residues are represented with as star (*) symbol and homologous residues are indicated using dot (.) symbol. The result thus obtained helps in improving the prediction of secondary and tertiary structure of proteins with a better understanding of weakly related proteins.

Target protein structure modeling

Protein 3D-structure prediction of PfCS modelled with both Modeller9v7 and Itasser. The modeled structure of PfCS can help us to know the mechanism of this enzyme action. CS protein monomer possess a novel "β-α-β sandwich fold." The active site of bound FMN is formed by the clustering of highly conserved regions along with certain flexible loops. Bound FMN has an isoalloxazine ring which is non-planar. Substrate binding site is generally targeted by drug compounds that disintegrates the chorismate product formation leading to folate reduction affecting the parasites growth.

Model validation

All the predicted models were validated with PROCHECK and ProsA program (Table 2). Comparing with Itasser server, Modeller9v7 predicted a good model for PfCS. Only the residues present in loop regions appeared in the disallowed region of the Ramachandran plot. PROSA plots depict the stability level of our model (Fig. 3).

Optimizing modeled structures using MD simulation

Energy minimization and MD simulation of the FMN bound CS model was carried out with the GROMACS 4.5.4 package using the GROMOS96 43a1 force field. The energy of CS and CS-FMN model has converged at steepest descent below 10,000 steps (Fig. 4). MD simulation analysis of root mean square deviation, potential energy, total energy, number of hydrogen bonds (NH) was done to explore the dynamic behavior of modeled protein. The hydrogen bond plot shows the binding affinity between CS protein and co-factor redFMN which retains four hydrogen bonds throughout the MD simulation process (1 ns) except 300 ps.

Secondary structure prediction

Secondary structure of protein were also predicted (Fig. 5) as they are highly conserved than amino acid sequence, which may help to understand more about the structure of modeled protein.

Active site prediction

Q-site finder tool is used for predicting ten possible ligand binding sites. The first active site from Q-site finder was chosen for this docking study. The selected active site residues are conserved and functionally active which present in the primary sequence of PfCS. Fig. 6 represents residues at the active site which includes Lys60, Glu86, Arg123, Lys122, Gly120, Arg46, Il332, Pro333, Arg483, Lys336, Leu400, Ser125, Gly126, Ile129, His184, Gly105, and Ser161.

Molecular docking

The high throughput virtual screening method was used to identify compounds with a favorable binding affinity toward ON and OFF state of CS protein (Muegge and Oloff, 2006). The grid parameter file was prepared and used for both ON and OFF condition of PfCS protein during molecular docking using AutoDock Vina. AutoDock doesn't calculate the non-covalent bond interactions which use only empirical scoring functions. Hence the ligands with high binding energy ranging from −10 to −8 Kcal/mol were selected for the first step of the screening process. Thus, 80 compounds among 240 compounds were selected for further study (Supplementary Table 1).

Potential lead identification

Drug likeliness and bioactivity prediction

Of 80, 34 compounds were found to follow drug likeliness properties. Fig. 7 shows the correlation between XlogP and TPSA. From 34

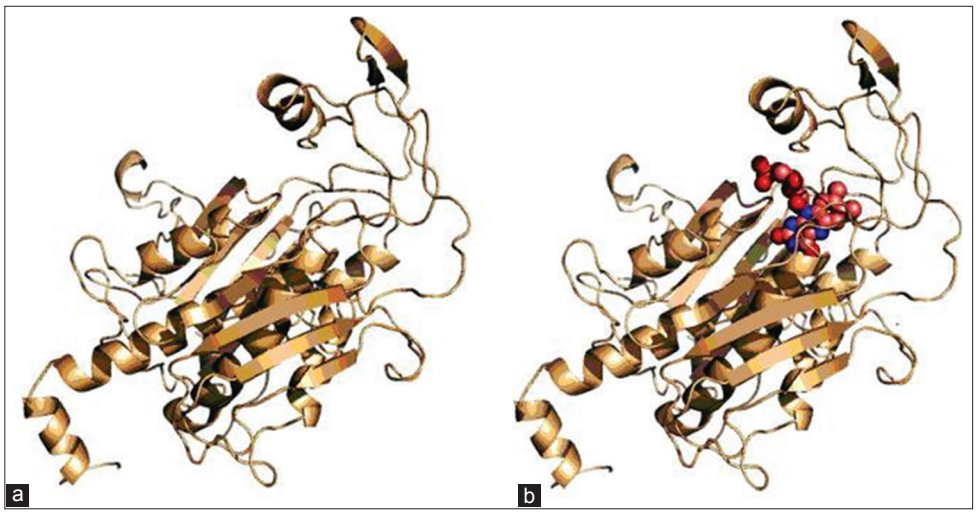

Fig. 2: Three-dimensional modeled structure of target protein, (a) Inactive form (OFF-state) of chorismate synthase (CS) protein structure, (b) active form (ON-state) of CS protein structure (CS with reduced flavin mononucleotide)

Table 2: Structure validation results of constructed CS models

Protein models	Template ID	Identity (%)	Tool	PROCHECK			
				a	b	c	d
PfCS protein	IR52 4LJ2 IUM0	46 43 41	Modeller 9v7	82.3	12.2	3.0	2.6
PfCS protein bound with redFMN	IR52 4LJ2 IUM0	46 43 41	Modeller 9v7	78.8	14.7	3.8	2.6
PfCS protein	-		Itasser	76.5	16.2	4.9	2.4

a: Percentage of residues in most favoured region, b: Percentage of residues in additionally allowed region, c: Percentage of residues in generously allowed region
d: Percentage of residues in disallowed region, *PfCS: Plasmodium falciparum* chorismate synthase, FMN: Flavin mononucleotide

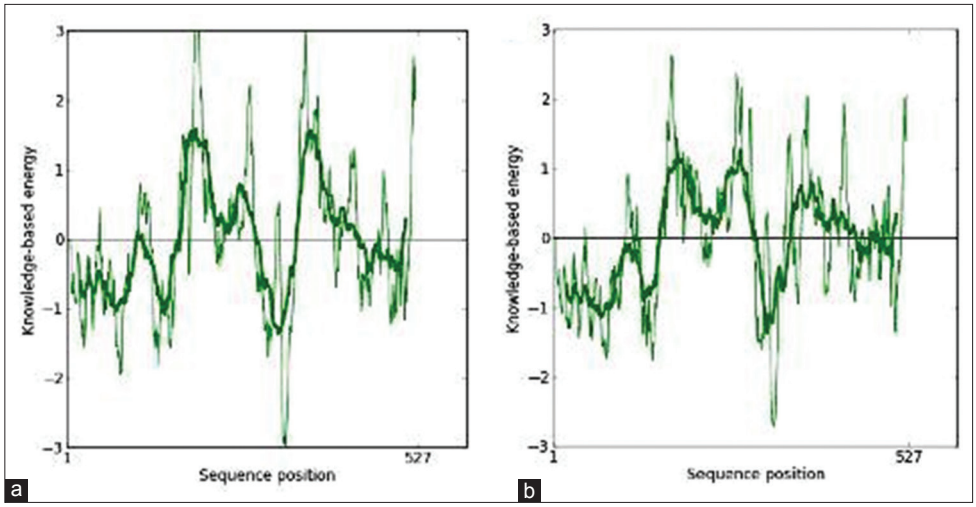

Fig. 3: Model validation plots of active (a) and inactive (b) form of chorismate synthase protein using ProsA server

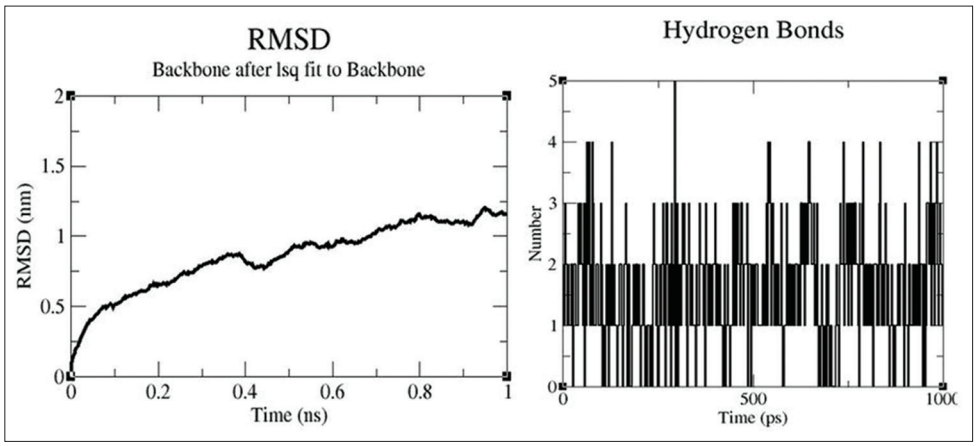

Fig. 4: Root mean square deviation plot and hydrogen bond plot using molecular dynamics simulation of chorismate synthase

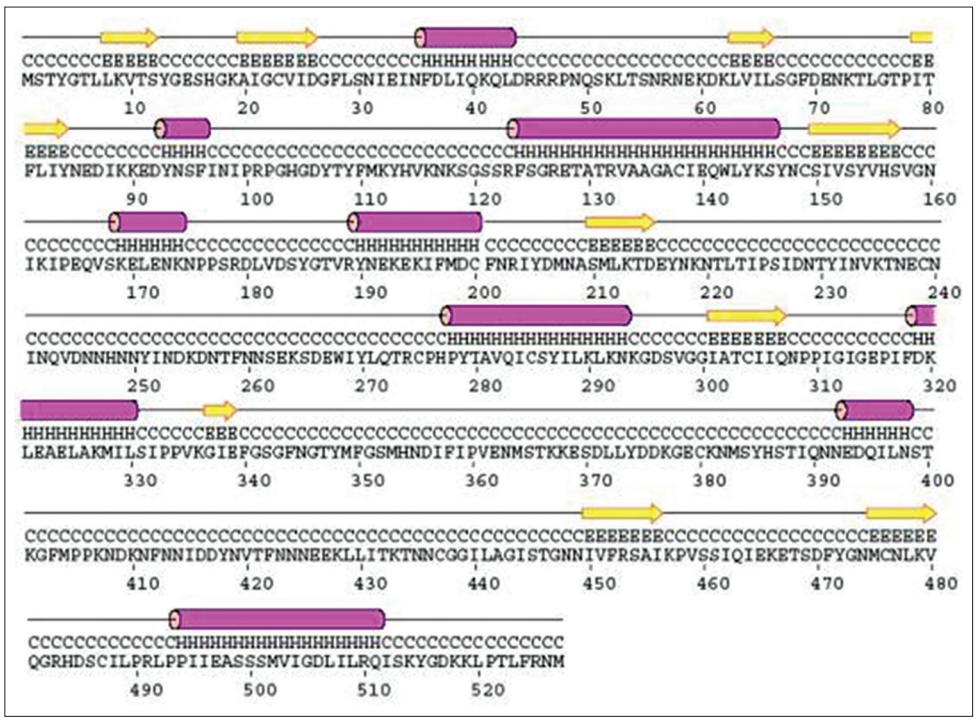

Fig. 5: Secondary structure prediction of chorismate synthase protein. Pink indicates helix; yellow indicates sheet; black line indicates coil

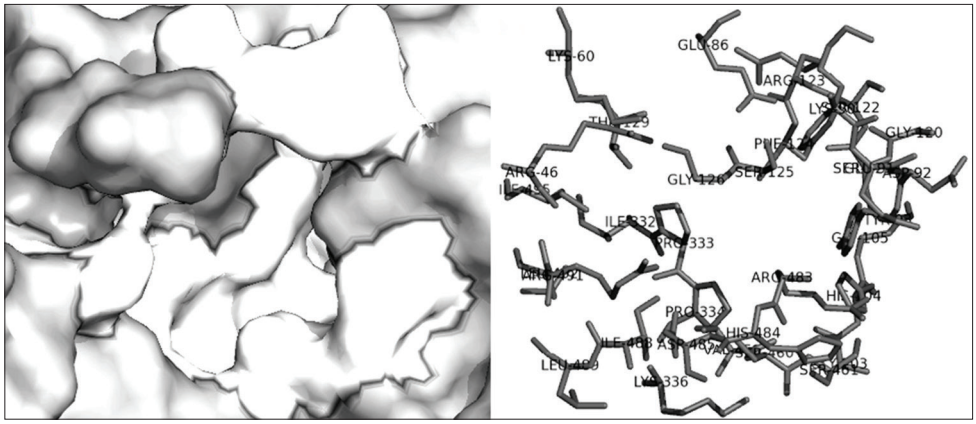

Fig. 6: Surface representation of binding pockets. Grey indicates the target protein; white indicates the ligand binding groove in target protein

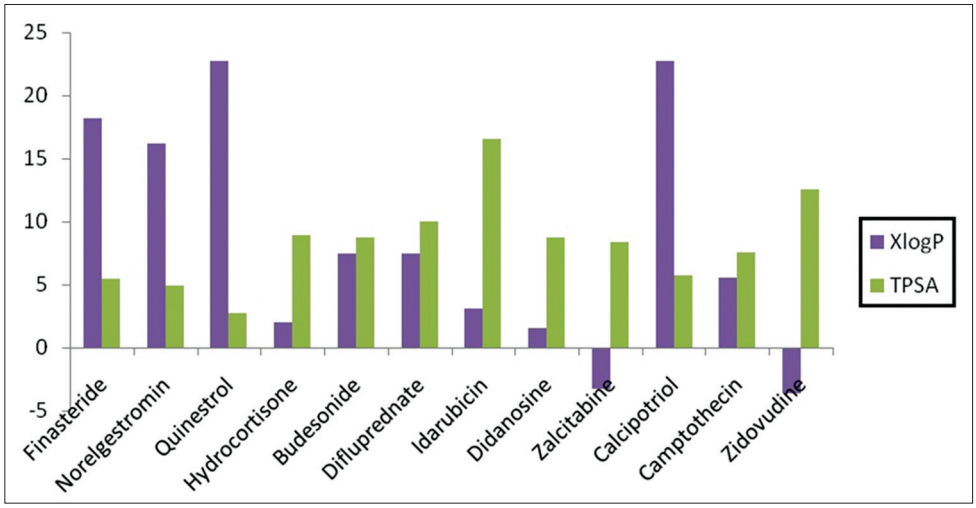

Fig. 7: Correlation between XlogP and topological polar surface area

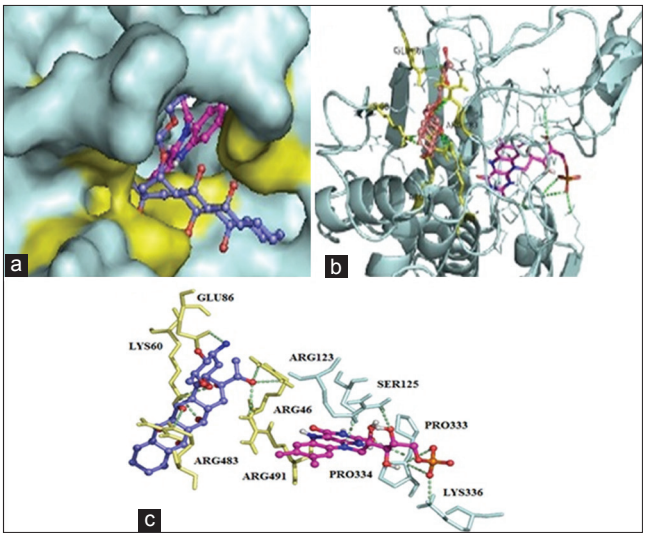

Fig. 8: Protein-ligand interaction of chorismate synthase (CS) protein with cofactor flavin mononucleotide-red (FMN) (active form), (a) Surface representation of CS-FMN with ligand, (b) ribbon schematic representations of CS-FMN with ligand, and (c) two-dimensional plot of protein-drug interaction

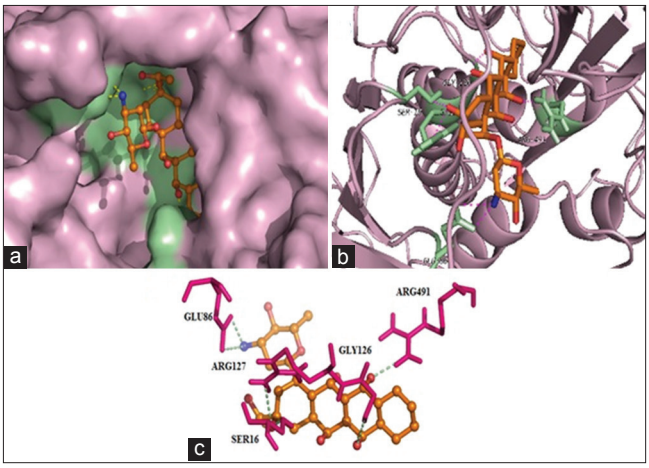

Fig. 9: Protein-ligand interaction of chorismate synthase (CS) protein without cofactor flavin mononucleotide-red (FMN) (inactive form), (a) Surface representation of CS with ligand, (b) ribbon schematic representations of CS with ligand, and (c) two-dimensional plot of protein-drug interaction

compounds, 12 compounds were screened based on rate of enzyme inhibitor value (more than 0.5) were taken for further analysis. (Table 3). Among 12 compounds, camptothecan, didanosine, zalcitabine, zidovudine, idarubicin, hydrocortisone, are act as lead like molecule. Finally, idarubicin identified as a potential antimalarial drug which is the only one compound shows anti-parasitic and anti-protozoan activity using PASS prediction server.

Table 3: The physiochemical properties of ligand molecules

Ligand name	Docking energy		miLogP	TPSA	MW	NHA	NHD	nRotB	XlogP	Volume	Enzyme inhibitor
	ON state	OFF State									
Finasteride	−11.6	−12.8	3.996	58	372.6	4	2	2	4.65	376.721	0.5
Norelgestromin	−13.3	−14.9	4.015	53	327.5	3	2	1	4.14	326.334	0.52
Quinestrol	−11.3	−12.5	5.596	29	364.5	2	1	2	5.83	364.834	0.56
Hydrocortisone	−12.5	−12.8	1.617	95	362.5	5	3	2	0.52	343.063	0.63
Budesonide	−13.3	−13.7	3.186	93	430.5	6	2	4	1.91	403.004	0.67
Difluprednate	−11	−11.5	3.922	107	508.6	7	1	8	1.90	453.067	0.7
Idarubicin	−13.7	−15.2	0.886	177	497.5	10	6	3	0.79	425.376	0.73
Didanosine	−9.8	−10	−0.947	93	236.2	7	2	2	0.40	199.28	0.79
Zalcitabine	−9	−9.1	−1.057	90	211.2	6	3	2	−0.84	185.748	0.85
Calcipotriol	−11.8	−11.6	4.594	61	412.6	5	3	5	5.82	421.938	0.93
Camptothecin	−13.5	−13	2.028	81	348.4	6	1	1	1.42	297.41	1.11
Zidovudine	−9.2	−11.1	−0.099	134	267.2	9	2	3	−0.93	224.063	1.17

*Bolded properties indicate lead molecules. nRotB: Number of rotatable bonds, TPSA: Topological polar surface area, MW: Molecular weight

Protein-ligand interaction analysis

All the compounds were successfully docked into the active site of CS protein (Supplementary Table 1). In that, FMN binding residues of CS active site pocket are highly conserved. Flexible loops of the enzyme contribute a major role in creating the active site pocket to which cofactor gets bound through non-covalent bonds. The residues of five major flexible loops that form FMN binding pocket are Arg46, Arg123, Ser125, Pro333, Pro334, Lys336 and Arg491. Highly conserved Ser125 in the active site pocket contributes to make stable interaction with isoalloxazine ring of FMN. However, Arg123 interacts with hydroxyl group and Lys336, Pro333, Pro334 interact with the phosphate group of ribityl chain of FMN. Arg491 which is a highly conserved amino acid in CS was found to contribute any interaction with the active site of generated model. In the ON state, the selected compound prefers substrate binding site (Fig. 8). The ligand idarubicin founds to interact with Arg46, Lys60, Glu86, Arg483, and Arg491.

CS protein is an apoenzyme in which FMNred absent in OFF state. In OFF state also idarubicin compound prefer the same binding site. It will interact with Ser16, Glu86, Gly126, Arg127, and Arg491 (Fig. 9). In the present study, the molecular model of PfCS constructed using crystal structure of known organism. The model also facilitated the recognition of conserved residues in active site pocket. The models study highly focused of the binding efficiency of all the ligands with inhibitory capacity against PfCS.

CONCLUSION

The shikimate pathway of PfCS enzyme, which is an apoenzyme that undergo catalysis in the presence of FMN, EPSP and chorismic acid. Hence, CS can be an important disease target for anti-malarial drugs. In this study, 3D structures (ON and OFF state) of the PfCS were modeled using Modeller9v7 software and optimized through molecular dynamic simulation studies using GROMACS software. Secondary structure predictions of modeled CS structures were also done with a view of having better understanding of the modeled structures. This gives a similar picture to that of CS from other organisms. The conserved residues present in the primary sequence were considered as active site residues for docking studies. Physiochemical properties, bio-active spectrum and drug likeliness were considered as the virtual screening filters that provided potency towards ligand selection for the target protein. From our findings through drug-target interaction studies, idarubicin compound has been identified as the potent inhibitor of PfCS protein. As the degree of drug resistance of the virus continues to be a frightening fact, this study has widened the scope of developing idarubicin based compounds as promising antibacterial agents.

ACKNOWLEDGMENTS

Authors are thankful to VIT University, Vellore for the computational facility and their continuous support and encouragement.

REFERENCES

1. Jana S, Paliwal J. Novel molecular targets for antimalarial chemotherapy. Int J Antimicrob Agents 2007;30(1):4-10.
2. Ludin P, Woodcroft B, Ralph SA, Mäser P. In silico prediction of antimalarial drug target candidates. Int J Parasitol Drugs Drug Resist 2012;2:191-9.
3. Fidock DA, Rosenthal PJ, Croft SL, Brun R, Nwaka S. Antimalarial drug discovery: efficacy models for compound screening. Nat Rev Drug Discov 2004;3(6):509-20.
4. Arcuri HA, Palma MS. Understanding the structure, activity and inhibition of chorismate synthase from *Mycobacterium tuberculosis*. Curr Med Chem 2011;18(9):1311-7.
5. Tapas S, Kumar A, Dhindwal S, Preeti, Kumar P. Structural analysis of chorismate synthase from *Plasmodium falciparum*: a novel target for antimalaria drug discovery. Int J Biol Macromol 2011;49:767-77.
6. Lindner J, Meissner KA, Schettert I, Wrenger C. Trafficked proteins-druggable in *Plasmodium falciparum*? Int J Cell Biol 2013;2013:435981.
7. Viola CM, Saridakis V, Christendat D. Crystal structure of chorismate synthase from *Aquifex aeolicus* reveals a novel beta alpha beta sandwich topology. Proteins 2004;54(1):166-9.
8. Arora N, Chari UM, Banerjee AK, Murty U. A computational approach to explore *Plasmodium falciparum* 3D7 chorismate synthase. Int J Genomics Proteomics 2007;3(1):3-28.
9. Quevillon-Cheruel S, Leulliot N, Meyer P, Graille M, Bremang M, Blondeau K, *et al*. Crystal structure of the bifunctional chorismate synthase from *Saccharomyces cerevisiae*. J Biol Chem 2004;279(1):619-25.
10. Ahn HJ, Yoon HJ, Lee B nd, Suh SW. Crystal structure of chorismate synthase: a novel FMN-binding protein fold and functional insights. J Mol Biol 2004;336(4):903-15.
11. Fitzpatrick T, Ricken S, Lanzer M, Amrhein N, Macheroux P, Kappes B. Subcellular localization and characterization of chorismate synthase in the apicomplexan *Plasmodium falciparum*. Mol Microbiol 2001;40(1):65-75.
12. Thompson JD, Higgins DG, Gibson TJ. CLUSTAL W: improving the sensitivity of progressive multiple sequence alignment through sequence weighting, position-specific gap penalties and weight matrix choice. Nucleic Acids Res 1994;22(22):4673-80.
13. Sali A, Blundell TL. Comparative protein modelling by satisfaction of spatial restraints. J Mol Biol 1993;234(3):779-815.
14. Laskowski RA, MacArthur MW, Moss DS, Thornton JM. PROCHECK: A program to check the stereochemical quality of protein structures. J Appl Crystallogr 1993;26:283-91.
15. Wiederstein M, Sippl MJ. ProSA-web: interactive web service for the recognition of errors in three-dimensional structures of proteins. Nucleic Acids Res 2007;35(Web Server issue):W407-10.
16. Hess B, Kutzner C, Van der Spoel D, Lindahl E. GROMACS 4: Algorithms for highly efficient, load-balanced, and scalable molecular simulation. J Chem Theory Comput 2008;4:435-47.
17. Trott O, Olson AJ. AutoDock Vina: improving the speed and accuracy of docking with a new scoring function, efficient optimization, and multithreading. J Comput Chem 2010;31(2):455-61.
18. DeLano WL. The PyMOL Molecular Graphics System. San Carlos, CA: DeLano Scientific LLC; 2002.

19. Lipinski CA, Lombardo F, Dominy BW, Feeney PJ. Experimental and computational approaches to estimate solubility and permeability in drug discovery and development settings. Adv Drug Deliv Rev 2001;46(1-3):3-26.
20. Wager TT, Chandrasekaran RY, Hou X, Troutman MD, Verhoest PR, Villalobos A, *et al*. Defining desirable central nervous system drug space through the alignment of molecular properties, *in vitro* ADME, and safety attributes. ACS Chem Neurosci 2010;1(6):420-34.
21. Muegge I, Oloff S. Advances in virtual screening. Drug Discov Today Technol 2006;3:405-11.
22. Filimonov D, Poroikov V. Bioactive Compound Design: Possibilities for Industrial Use. PASS: Computerized Prediction of Biological Activity Spectra for Chemical Substances. Portsmouth, UK: BIOS Scientific Publishers; 1996. p. 44-56.

Supplementary table 1: Binding score of all the ligands in both ON and OFF state pfCS protein

Compound name	Docking energy		Compound name	Docking energy	
	OFF-state	ON-state		OFF-state	ON-state
Compound 9	−11.3	−9.7	Anisotropine Methylbromide	−7.5	−7.1
Cyclosporine	−13.2	−10.7	Cromoglicic acid	−12.7	−11.3
Cyanocobalamin	−14.3	−13.4	Afatinib	−10.8	−9.3
Pyruvic acid	−5	−4.4	Zidovudine	−11.1	−9.2
Choline	−4.3	−4.7	Isosorbide Mononitrate	−7.7	−7.3
Vitamin C	−7.4	−7.2	Selegiline	−6.8	−7
Spermine	−6	−4.8	Hydroxystilbamidine Isethionate	−7	−6.8
L-Cystine	−6.1	−6.2	Thalidomide	−11.2	−9.8
Thiamine	−8.2	−7.3	Novobiocin	−11.5	−10
Lipoic Acid	−6.1	−5.8	Tocainide	−8	−7.2
Pravastatin	−7.7	−7	Glipizide	−11.2	−10
Masoprocol	−9.7	−9.2	Pilocarpine	−7.3	−6.9
Amphetamine	−7.4	−6.6	Primaquine	−8	−7.2
Tramadol	−9.7	−7.8	Leflunomide	−9.9	−10
Caffeine	−7.8	−7.7	Rosuvastatin	−9.1	−8.1
Pyrimethamine	−9.4	−8.3	Capecitabine	−9.1	−8.6
Adapalene	−13.8	−11.6	Quinacrine	−7.4	−8.4
Citalopram	−11.3	−7.9	Sibutramine	−8.2	−7.4
Indinavir	−12.2	−10.8	Atovaquone	−13.5	−12.2
Lovastatin	−8.9	−7.6	Dutasteride	−15.7	−12.9
Enflurane	−6.8	−7.5	Proguanil	−7.7	−6.9
Pregabalin	−6	−5.9	Bretylium	−6.8	−6.2
Nevirapine	−10.2	−8.8	Calcium Chloride	−6	−5.8
Calcium Acetate	−7.6	−7	Guanethidine	−8.2	−6.9
Dicoumarol	−14.1	−11.4	Idarubicin	15.2	−13.7
Acarbose	−12.5	−11.4	Podofilox	−11.5	−9.2
Etomidate	−6.7	−6.7	Ifosfamide	−7	−5.9
Tolcapone	−9.9	−8.8	Ciclopirox	−10.2	−8.7
Salbutamol	−8	−7.6	Acebutolol	−7.9	−7.4
Alfuzosin	−11.1	−9	Lomustine	−7.3	−6.9
Thioguanine	−7.2	−7.3	Clarithromycin	−12.1	−12.4
Aztreonam	−10	−7.7	Finasteride	−12.8	−11.6
Chlorzoxazone	−8.1	−6.5	Halofantrine	−10.2	−9.3
Mefloquine	−11.4	−9.8	Budesonide	−13.7	−13.3
Mirtazapine	−13.1	−10.7	Chloroxine	−9	−7.4
Amlodipine	−8.9	−7.6	Iodixanol	−10.7	−8.1
Nimodipine	−9.1	−7.9	Posaconazole	−10.8	−10.3
Nisoldipine	−9.5	−7.7	Varenicline	−9.2	−7.7
Alprazolam	−11.6	−9.7	Vecuronium	−12.3	−10.7
Loxapine	−11.8	−9.6	Dihydroxyaluminium	−7.2	−7
Acetohexamide	−8.8	−9.2	Magnesium oxide	−2.5	−2.3
Hyoscyamine	−10	−7.5	Salsalate	−9.3	−8
Famciclovir	−8.3	−7.5	Ciclesonide	−14.5	−13.7
Lindane	−8.2	−7.4	Oxybenzone	−8.7	−8
Nitric Oxide	−3	−3	Bezitramide	−11.3	−10.6
Trimethoprim	−8.5	−7.6	Diethyltryptamine	−8.6	−7.3
Epirubicin	−14.1	−13	Alpha−ethyltryptamine	−8.8	−7.2
Dipivefrin	−8.8	−7.7	Bromazepam	−10.3	−8.1
Prazosin	−12.2	−9.7	Cilastatin	−8.4	−8
Acitretin	−11.5	−8.7	Tazobactam	−9.3	−7.5
Nabumetone	−10.3	−8.3	Hydroxychloroquine	−9.3	−7.6
Quinine	−10.2	−9.3	Erythrityl Tetranitrate	−7.3	−6.4
Dronabinol	−11	−10.6	Molindone	−9.4	−9.6
Entacapone	−8.5	−7.7	Dithioerythritol	−4.8	−3.2
Dextromethorphan	−11.8	−11.5	Dihydroxyacetone	−10.4	−4.2
Cisplatin	−6.5	−6.2	Piclamilast	−11.3	−8.3
Balsalazide	−10.8	−10	Compound 12	−10.4	−9.9
Trandolapril	−8.3	−8.4	Benzophenone	−10.1	−8.3
Erlotinib	−9.6	−7.8	(Aminooxy)Acetic Acid	−4.9	−4.5

Contd...

Supplementary table 1: Contd...

Compound name	Docking energy		Compound name	Docking energy	
	OFF-state	ON-state		OFF-state	ON-state
Chlormerodrin	−5.9	−5	Isatin	−8.8	−7.8
Gadoversetamide	−6.3	−6	Calcipotriol	−11.6	−11.8
Methoxsalen	−9	−8.4	Compound 19	−11.8	−9.6
Bosentan	−10.8	−8.9	Novo Nordisk a/S Compound	−9.3	−6.8
Propranolol	−8.7	−7.6	Cyanamide	−3	−2.6
Valaciclovir	−9.1	−8.3	Nicotinamide	−6.6	−6.2
Doxazosin	−13.5	−11	Compound 18	−10.7	−10.4
Piperazine	−4.2	−3.9	Phosphonoacetic Acid	−5.6	−5.4
Amiloride	−8.9	−8.1	Frovatriptan	−9.9	−8.8
Sulindac	−11	−9.3	Quisqualate	−7.7	−7.1
Chloroquine	−8.1	−6.7	Beta−Alanine	−4.6	−4.1
Amodiaquine	−9.8	−9.8	Phenol	−6.5	−5.8
Imatinib	−12.8	−9.7	Pyruvoyl Group	−4.3	−3.9
Leucovorin	−10.6	−10.4	Butylamine	−4.2	−3.9
Isoflurophate	−6.2	−5.1	Adenosine−5'−Phosphosulfate	−11	−8.9
Losartan	−10.7	−9.1	Compound 4−D	−11.7	−9.9
Midazolam	−11.7	−9.8	Benzoic Acid	−7.5	−8.8
Pomalidomide	−11.8	−9.8	Formaldehyde	−2.2	−1.9
Fluorescein	−16.8	−12.7	Eucalyptol	−9.8	−11.1
Diethylcarbamazine	−7.1	−6.8	Urea	−4	−3.5
Paroxetine	−11	−9.4	Compound 5	−10.7	−9.7
Nitroglycerin	−6.9	−5.7	Trametinib	−12.4	−10.7
Nateglinide	−9.1	−8.6	Citric Acid	−5.9	−5.4
Pralidoxime	−7	−6.8	Trimethyl Glycine	−4.7	−5.1
Esomeprazole	−11	−9.6	Trioxsalen	−12.1	−9.7
Hydrocortisone	−12.8	−12.5	Quinestrol	−12.5	−11.3
Hexachlorophene	−10.6	−9.7	Aniracetam	−8.2	−7.3
Clopidogrel	−9.4	−7.1	Dibromothymoquinone	−7.9	−9.1
Benzquinamide	−9.8	−8.5	Camptothecin	−13	−13.5
Malathion	−6.3	−5.3	4−Butyrolactone	−5	−5.6
Roxithromycin	−13.7	−10.6	Suramin	15.5	−10.1
Bedaquiline	−12.5	−9.6	Zimelidine	−9.1	−7.1
Phenylbutazone	−9.7	−9.1	Dronedarone	−8.1	−7.4
Meloxicam	−11.5	−9.6	Voacamine	−14.8	−13.1
Menthol	−9.1	−7.3	Voglibose	−7.9	−7.3
Phenmetrazine	−7.6	−7.4	Ospemifene	−9.3	−7.7
Mifepristone	−13.7	−11	Iloperidone	−11.6	−10
Aminolevulinic acid	−5.5	−5.7	Indacaterol	−13.5	−10.2
Sirolimus	−18	−14	Mianserin	−13.3	−10.8
Isosorbide Dinitrate	−8	−7.4	Acetylcysteine	−5.4	−5.8
Didanosine	−10	−9.8	Alogliptin	−10.7	−8.6
Methdilazine	−11.2	−10.1	Vilazodone	−12.8	−10.9
Ethacrynic acid	−8.1	−7.4	Mevastatin	−9.7	−8.9
Bimatoprost	−9	−8.4	Artemether	−10.8	−7.9
Buprenorphine	−13.3	−11.5	Norelgestromin	−14.9	−13.3
Levosimendan	−9.6	−8.7	Aluminum hydroxide	−6	−5.7
Salicyclic acid	−7.5	−6.9	Aniline	−6.5	−7.6
Zalcitabine	−9.1	−9	Difluprednate	−11.5	−11
Acetylsalicylic acid	−7.9	−9.2	Nepafenac	−9.4	−8.4
Rizatriptan	−9.1	−7.3	Metiamide	−6	−5.3
Dirithromycin	−12.7	−10.5	Tofisopam	−9.4	−7.6
Carboplatin	−7.1	−6.9	Spinosad	−12.4	−11.3
Telmisartan	−9.9	−10.6	Fidaxomicin	−14.1	−10.8
Dactinomycin	−15.4	−13	Vemurafenib	−9.8	−10.5
Edetic Acid	−6.8	−5.1	Gadoxetate	−6.5	−6.1
Ramelteon	−11	−9	Regorafenib	−13.1	−9.8
Cytarabine	−9.4	−8.7	Enzalutamide	−11.7	−9.8
Azathioprine	−9	−7.3	Ipratropium bromide	−7.9	−7.3
Auranofin	−7.2	−7	Gadopentetate dimeglumine	−6.9	−6.5
Gabapentin	−8.2	−6.1	Pentosan Polysulfate	−10.3	−9.6
3'-Phosphate-Adenosine-5'-Phosphate Sulfate	−9.9	−9.2	N−(Allyloxycarbonyl)−4−[N−(Carboxy−Formyl)−2−(Benzoic Acid)−Amino]−L−Phenylalaninyl−Amino−Butyloxy−(6−Hydroxy−Benzoic Acid Methyl Ester)	−9.6	−8.2